

# Robust and Stable Periodic Flight of Power Generating Kite Systems in a Turbulent Wind Flow Field

Julia Sternberg\* Jay Goit\*\* Sébastien Gros\* Johan Meyers\*\*  
Moritz Diehl\*

\* Optimization in Engineering Center (OPTEC), Department of Electrical Engineering, K.U. Leuven, Kasteelpark Arenberg 10, B-3001 Leuven-Heverlee, Belgium (e-mail: julia.sternberg@esat.kuleuven.be, sgros@esat.kuleuven.be, moritz.diehl@esat.kuleuven.be).

\*\* Optimization in Engineering Center (OPTEC), K.U. Leuven, Department of Mechanical Engineering, K.U. Leuven, Celestijnenlaan 300 A, B3001 Leuven, Belgium (e-mail: jay.goit@mech.kuleuven.be, johan.meyers@mech.kuleuven.be)

---

**Abstract:** Power-generating kite systems extract energy from the wind by periodically pulling a generator on the ground while flying fast in a crosswind direction. Kite systems are intrinsically unstable, and subject to atmospheric turbulences. As an alternative to closed-loop control, this paper investigates the open-loop stabilization and robustification of a kite system using techniques based on the solution of Lyapunov differential equation. A wind flow is computed as a solution to a time-dependent three dimensional Navier-Stokes equation. Open-loop stable trajectories for the power-generating kite system are computed based on the statistical properties of the wind field, and are robustified with respect to the system constraints. The stability and robustness of the resulting trajectories are assessed by simulating the system using the computed time- and space-dependent turbulent wind flow.

*Keywords:* Optimal control, kite systems, open-loop control, robust control, turbulent wind flow.

---

## 1. INTRODUCTION

The idea of using kites for power generation has originally been proposed by Loyd (1980). Power-generating kite systems are currently the object of academic and industrial research (see Canale et al. (2006); Lansdorp and Ockels (2005); Ockels et al. (2006); Williams et al. (2008) and the references therein for an overview). Power can be generated by a) performing a cyclical variation of the tether length, together with cyclical variation of the tether tension, reeling a generator fixed to the ground, or b) by using on-board turbine(s), transmitting the power to the ground via the tether. In this paper, the first option is considered.

An important challenge for the control of power-generating kites is that the system dynamics are unstable and strongly affected by atmospheric turbulences, which are stochastic and very unpredictable. Closed-loop control is a natural choice to stabilize power-generating kite systems, however closed-loop control makes the safety of the technology critical to sensors and actuators faults. Open-loop stability of power-generating kite systems, if it can be achieved, is therefore an attractive alternative to closed-loop control. It is also useful in combination with closed-loop control in order to improve the safety of the system.

Power-generating kite systems are subject to operational constraints. Hence if operated in open-loop, the system trajectories must not only achieve stability but also achieve the robustness of the system constraints with respect to disturbances. Most existing stability optimization techniques are either based on

the optimization of the asymptotical decay rate of the system, the optimization of the so called pseudo-spectral abscissa, or on the smoothed spectral abscissa or radius. Robust optimization approaches for non-linear systems are commonly based on linear approximations techniques Diehl et al. (2006b); Houska and Diehl (2009); Nagy and Braatz (2004).

This paper builds on the methods developed in Houska and Diehl (2010) using a more realistic wind field generated by a computational fluid dynamic (CFD) simulation. The statistical properties of the wind field are computed based on the wind field obtained in the CFD simulation, which are used to compute the open-loop stable and robust trajectories. The stability and robustness of the resulting trajectories are assessed in simulation.

The paper is organized as follows: In Section 2 a brief model description for power generation with kites based on crosswind flight is given. Moreover, an optimal control problem for finding periodic trajectories that maximize the power production, is formulated. Also, in Section 2 it is described how to compute the time- and space-dependent turbulent wind flow using a CFD simulation code from KU Leuven. In Section 3 we discuss the stability and robustness properties of computed trajectories and explain some numerical techniques which help us to stabilize and robustify trajectories. We particularly employ techniques based on Lyapunov differential equations. After that, in Section 4, the optimal a-priori stable and robust kite trajectories are simulated considering a realistic time- and space-dependent wind profile characterized by unknown turbulences. The be-

haviour of the kite influenced by this flow field is studied. In the last Section 5 of this paper some concluding remarks are given.

The main contributions can be summarized as follows: In this paper we present some new robust and open-loop stable trajectories for a power generating kite system. Here the wind profile for the model is given by mean velocities of the turbulent time- and space-dimensional wind flow, which will be used for the post-processing simulation. Two different models for unknown wind disturbances are considered: a) uncorrelated white noise random process; b) uncorrelated bounded random process with turbulence intensities depending on the altitude.

The second contribution consists in testing the intrinsically open-loop stable and robust orbits simulating them in a time- and space-dependent turbulent wind flow.

## 2. MODEL DESCRIPTION, PROBLEM FORMULATION AND WIND FLOW COMPUTATION

### 2.1 Model description

This section provides a brief description of the kite system model. A more detailed overview can be found in Houska (2007); Houska and Diehl (2007, 2010). The system is considered in a 3-dimensional Euclidean space, so that the wind is blowing in the  $e_x$  and  $e_y$  directions only. The vector  $e_z$  points to the sky and  $e_y$  is defined by  $e_y := e_z \times e_x$ , such that  $\{e_x, e_y, e_z\}$  builds an orthonormal right-handed basis of the 3-dimensional Euclidean space. The generator is fixed at the origin of this coordinate system. Thus, the position  $p \in \mathbb{R}^3$  of the kite can be described by  $p = r e_r$ , where  $r$  stands for the tether length, i.e., the distance between the generator and the kite. The unit vector  $e_r$  is defined by  $e_r := (\sin(\theta) \cos(\phi), \sin(\theta) \sin(\phi), \cos(\theta))$ . Note that  $\phi = 0$  corresponds to the  $e_x$  direction. The angle  $\theta = 0$  corresponds to the zenith position, and  $\theta = \frac{\pi}{2}$  indicates that the kite touches the ground.

The control variables are: a) the second derivative of the tether length  $\ddot{r}$ ; b) the first derivative of the roll angle of the kite  $\dot{\psi}$ ; c) the first derivative of the lift coefficient  $\dot{C}_L$ . Vector  $\mathbf{u}$  consists of all the control variables, i.e.,  $\mathbf{u} = (\ddot{r}, \dot{\psi}, \dot{C}_L)$ . The steering of the system can be performed in the following manner: the length  $r$  of the tether can be controlled by the winch and the roll angle  $\psi$  by varying the difference between the lengths of the two tethers leading to the right and left wing tip of the kite. The lift coefficient  $C_L$  can be controlled by an elevator. This point model of the kite includes the physical equations for the lift and drag force (considering tether drag), and gravitational forces. Here, the orientation of the kite is computed under the assumption that the main axis is always in line with the effective wind i.e., a possible side slip is neglected.

### 2.2 Problem formulation

In this section the optimal control problem for finding periodic trajectories and maximizing the power produced, is formulated. The average power  $W$  at the generator can be computed as

$$W := \frac{1}{T} \int_0^T F_c \dot{r} dt,$$

where  $F_c > 0$  is the tether tension and  $T$  is the duration of the periodic trajectory. The dynamics of the kite system are described by the model equation  $\dot{\mathbf{x}}(t) = f(\mathbf{x}(t), \mathbf{u}(t), w(z, t))$ ,

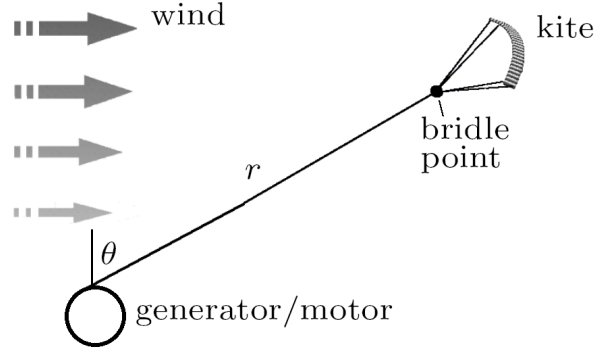


Fig. 1. Schematic illustration of a single kite system, Houska (2007)

Table 1. Parameters of the kite model

Dimension	Description [unit]	Value
$A_k$	wing surface area [ $\text{m}^2$ ]	500
$c_D$	aerodynamic drag coefficient [-]	0.04
$\rho$	air density [ $\text{kg}/\text{m}^3$ ]	1.23
$m$	kite mass [kg]	850
$\phi_l$	lower bound for $\phi$	-0.34
$\phi_u$	upper bound for $\phi$	0.34
$\theta_l$	lower bound for $\theta$	0.4
$\theta_u$	upper bound for $\theta$	1.45
$\psi_l$	lower bound for $\psi$	-0.29
$\psi_u$	upper bound for $\psi$	0.29
$C_{Ll}$	lower bound for $C_L$	0.1
$C_{Lu}$	upper bound for $C_L$	1.5
$\dot{\psi}_l$	lower bound for $\dot{\psi}$	-0.065
$\dot{\psi}_u$	upper bound for $\dot{\psi}$	0.065
$\dot{C}_{Ll}$	lower bound for $\dot{C}_L$	-3.5
$\dot{C}_{Lu}$	upper bound for $\dot{C}_L$	3.5
$\dot{r}_l$	lower bound for $\dot{r}$	-40
$\dot{r}_u$	upper bound for $\dot{r}$	10
$\ddot{r}_l$	lower bound for $\ddot{r}$	-25
$\ddot{r}_u$	upper bound for $\ddot{r}$	25

where all the state variables that characterize the position of the kite and its velocity are collected into the vector  $\mathbf{x}(t)$ , i.e.,  $\mathbf{x}(t) = (r, \phi, \theta, \dot{r}, \dot{\phi}, \dot{\theta})$ . The optimal control problem (OCP) for finding periodic trajectories and maximizing the power produced, can be formulated as

$$\begin{aligned} & \min_{\mathbf{x}(\cdot), \mathbf{u}(\cdot), T} J(T, \mathbf{x}(t)) \\ & \text{subject to:} \\ & \forall t \in [0, T] : \dot{\mathbf{x}}(t) = f(\mathbf{x}(t), \mathbf{u}(t), w(z, t)), \\ & \quad 0 \geq h(\mathbf{x}(t), \mathbf{u}(t)), \\ & \quad \mathbf{x}(0) = \mathbf{x}(T), \end{aligned} \quad (1)$$

with the objective function  $J(T, \mathbf{x}(t))$  defined as  $J(T, \mathbf{x}(t)) = -W$ . The periodicity of the kite orbit is guaranteed by the periodic constraints  $\mathbf{x}(0) = \mathbf{x}(T)$ . The function  $h(\mathbf{x}(t), \mathbf{u}(t))$  lumps together the system operational constraints and actuators limitation (cf. Table 1). Table 1 summarizes the choice of parameter values, that describe physical properties and constraints limitations for a particular kite system. The wind disturbances are described by the function  $w(z, t)$ , which are in our case time- and altitude-dependent.

### 2.3 Computation of time- and space-dependent three dimensional turbulent wind flow

In this section we discuss the time dependent flow field which is used first to compute, and second to simulate open-loop stable

and robust kite trajectories in a more realistic environment. Three dimensional flow field is generated from a boundary layer simulation. The instantaneous flow field is saved for every time step of the simulation. For the boundary layer simulation an in-house research code Calaf et al. (2010) is used. This code is based on large eddy simulation and solves the filtered Navier-Stokes equations, i.e.,

$$\begin{aligned} \frac{\partial \vec{v}}{\partial t} + \vec{v} \cdot \nabla \vec{v} &= -\frac{1}{\rho} \nabla p - \nabla \tau_{\text{sgs}} - f \vec{v} \times \mathbf{e}_z, \\ \nabla \cdot \vec{v} &= 0, \end{aligned} \quad (2)$$

where  $v$  stands for the filtered velocity field,  $p$  the pressure,  $\tau_{\text{sgs}}$  the subgrid-scale tensor and  $f = 10^{-4} \text{ sec}^{-1}$  is the Coriolis parameter at 43 degree latitude.

The KU Leuven code uses a pseudo-spectral discretization in the streamwise and spanwise directions and a fourth-order energy-conservative finite difference discretization in the vertical direction. As a result, horizontal boundary conditions are periodic. The top boundary condition is a zero vertical velocity, zero shear stress boundary. The bottom boundary condition uses Monin-Obukhov similarity theory to calculate filtered surface shear stress as a function of the velocity at the first vertical cell. Time advancement is performed using a four-stage fourth-order Runge-Kutta method and the code is fully dealiased using 3/2 rule.

The height of the computation domain is  $H = 2500$  m and therefore it is high enough for the kite flying at the height of approximately 500 – 1000 m. The domain spans a distance of  $L_x = 6280$  m and  $L_y = 3140$  m in horizontal directions. Number of grid points in these directions are  $N_x \times N_y \times N_z = 128 \times 192 \times 151$ . We save the complete flow field every three seconds.

The  $x$ -component of the wind velocity  $\vec{v}(\vec{x}, t) = (v_x, v_y, v_z)$  at the time point  $t = 3$  seconds is shown in Fig. 2.

### 3. STABLE AND ROBUST OPTIMAL CONTROL OF PERIODIC SYSTEMS

This section describes a methodology to compute open-loop stable and robust periodic trajectories for the OCP (1). Nominally optimized periodic orbits are presented in Section 3.1. In Section 3.2 an approach based on the solution of the periodic Lyapunov differential equation, which is used in order to find open-loop stable and robust trajectories, is briefly described. Section 3.3 and Section 3.4 discuss robustly optimized open-loop stable periodic orbits, considering two different models for unknown wind disturbances, respectively: a) uncorrelated white noise random process; b) uncorrelated bounded random process with turbulence intensities depending on the altitude.

It was already shown in Houska and Diehl (2010) that open-loop stable orbits exist in simulation for a large power-generating kite system with almost 2 km tether length and a kite with 500 m<sup>2</sup> wing area and 850 kg weight. A wind shear model was used and it was assumed that the wind blows in the  $x$ -direction only.

In the present paper we consider the more realistic wind profile computed in Section 2.3. The wind flow resulting from the CFD simulation provides a 3-dimensional wind profile, where a local wind velocity vector  $\vec{v}(\vec{x}, t) = (v_x, v_y, v_z)$  is defined as a function in space and time.

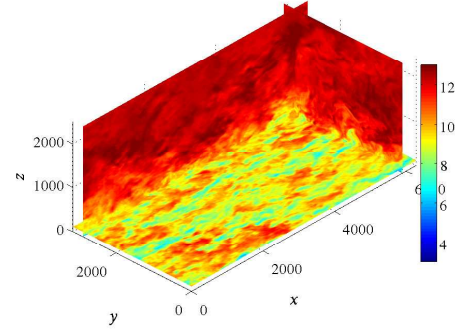


Fig. 2.  $v_x$  component of the wind velocity at the time point  $t = 3$

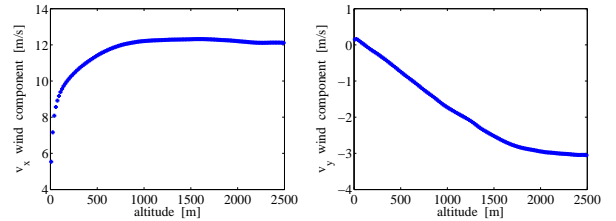


Fig. 3. Mean velocity profiles  $\bar{v}_x$  (left) and  $\bar{v}_y$  (right) of the wind speed in the atmospheric Ekman layer. (Note that  $\bar{v}_z = 0$ )

#### 3.1 Nominal periodic trajectory

In order to compute an open-loop stable and robust trajectory, a nominal periodic solution to problem (1) must be obtained, i.e., the OCP (1) is solved assuming that  $w(z, t) = 0$ . This means that the system has no disturbances. The mean-values  $(\bar{v}_x, \bar{v}_y, 0)$  of the local wind velocity  $\vec{v}(\vec{x}, t) = (v_x, v_y, v_z)$  are used for the nominal optimization, and are assumed to be functions of the altitude  $z$  only (see Fig. 3).

The nominal periodic kite trajectory was computed using the optimal control software ACADO Toolkit Houska et al. (2011). The locally optimal solution for the OCP (1) with no wind disturbances, i.e.,  $w(z, t) = 0$ , is shown in Fig. 4 (solid line).

Before we add some wind turbulences to the model and start to make the nominal optimal trajectory robust against them, the periodic solution in Fig. 4 has to be analysed regarding stability aspects, since stability is a necessary requirement for the robustification of the periodic solution.

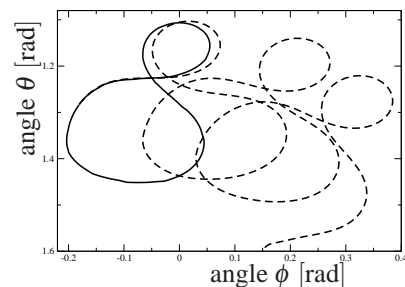


Fig. 4. Unstable kite trajectory: nominal solution (solid line) and simulated solution in presence of small perturbations of the wind profile (dashed line). The period is  $T = 19.6$ s.

The stability of the periodic solution of the optimal control problem (1) can be investigated by computing the spectral radius of the monodromy matrix  $X$ , defined as:

*Definition 1.* (Monodromy matrix). The monodromy matrix  $X$  is defined as  $X := Y(T, 0)$  where  $Y : \mathbb{R} \times \mathbb{R} \rightarrow \mathbb{R}^{n_x \times n_x}$  is the fundamental solution obtained as

$$\frac{\partial Y(t, \tau)}{\partial t} = \frac{\partial f}{\partial \mathbf{x}}(\mathbf{x}(t), \mathbf{u}(t), 0)Y(t, \tau) \quad \text{with} \quad Y(\tau, \tau) = 1$$

for all  $t, \tau \in \mathbb{R}$ .  $\square$

A periodic solution of a nonlinear differential system is intrinsically stable, if the spectral radius  $\rho$  of the monodromy matrix  $X$  is less than one. The spectral radius  $\rho$  of the monodromy matrix  $X$  associated with the solution from Fig. 4 is  $\rho = 1.2 > 1$ , and thus, the power optimal trajectory is unstable. The instability of the nominal solution to (1) can be illustrated via a simulation of the dynamic system in the presence of small perturbations of the wind profile. It can be seen in Figure 4 (dashed line) that in such a case the kite diverges quickly from the nominal solution and finally crashes after less than three periods.

### 3.2 Stable and robust optimal control based on periodic Lyapunov differential equation

In order to achieve stability of the periodic solution a feedback controller can be introduced (see e.g. Canale et al. (2007); Ilzhoefer et al. (2007), where a non-linear model predictive controller was used). In this paper, however, we are looking for open-loop stable trajectories which have several practical advantages, e.g. flying an open-loop stable trajectory the kite does not rely on sensors and actuators faults. Additionally, open-loop stable and robust orbits are also useful in combination with feedback control as tracking an inherently open-loop stable orbit is typically easier than tracking an unstable trajectory.

In order to guarantee first the open-loop stability of the system, and second its robustness w.r.t. the path constraints, an approach based on the Taylor expansion is employed, see Diehl et al. (2006a); Houska (2007); Houska et al. (2009); Nagy and Braatz (2004, 2007). In this paper we consider the first order approximations. Required sensitivities can be computed using the solution of the periodic Lyapunov differential equation

$$\begin{aligned} \dot{P}(t) &= A(t)P(t) + P(t)A(t)^\top + B(t)B(t)^\top, \\ P(0) &= P(T). \end{aligned} \quad (3)$$

We refer to Houska (2007); Houska et al. (2009) for a detailed description of this method. Once the solution  $P(t)$  of the periodic Lyapunov differential equation (3) is available, the first order approximation of the path constraints  $h(\mathbf{x}(t), \mathbf{u}(t))$  can be calculated as

$$\tilde{h}_i(\mathbf{x}(t), \mathbf{u}(t)) = h_i + \gamma \sqrt{\frac{\partial h_i}{\partial \mathbf{x}}^\top P(t) \frac{\partial h_i}{\partial \mathbf{x}}},$$

where  $\gamma \geq 0$  is a confidence-level parameter. Using the following lemma, we can guarantee the existence and uniqueness of the periodic solution for the Lyapunov differential equation, provided that the system is asymptotically stable:

*Lemma 1.* (Lyapunov Lemma, cf. Bolzern and Colaneri (1988)). The periodic Lyapunov differential equation admits a unique  $T$ -periodic and positive definite solution  $P(t) \succ 0$  if and only if the monodromy matrix  $X := Y(T, 0)$  is asymptotically stable (all eigenvalues are contained in the open unit disc) and the

reachability Grammian matrix  $Q(T)$  is positive definite. The reachability Grammian matrix  $Q(T) \in \mathbb{R}^{n_x \times n_x}$  is defined as

$$Q(T) := \int_0^T Y(T, \tau)B(\tau)B(\tau)^\top Y(T, \tau)^\top d\tau. \quad \square$$

The robust counterpart of the OCP (1) using the periodic Lyapunov differential equation to compute sensitivities can be formulated as

$$\begin{aligned} \min_{\mathbf{x}(\cdot), \mathbf{u}(\cdot), P(\cdot), T, \gamma} \quad & -\gamma \\ \text{s.t.} \quad & \end{aligned} \quad (4)$$

$$\dot{\mathbf{x}}(t) = f(\mathbf{x}(t), \mathbf{u}(t), 0), \quad \forall t \in [0, T], \quad (5)$$

$$\dot{P}(t) = A(t)P(t) + P(t)A(t)^\top + B(t)\Sigma B(t)^\top, \quad (6)$$

$$\mathbf{x}(0) = \mathbf{x}(T), \quad P(0) = P(T), \quad (7)$$

$$0 \geq h_i(\mathbf{x}(t), \mathbf{u}(t)) + \gamma \sqrt{C^i(t)P(t)C^i(t)^\top}, \quad (8)$$

$$J(T, \mathbf{x}(T)) \geq 0.8 J_{\text{nominal}}(T, \mathbf{x}(T)), \quad (9)$$

$$A(t) := \frac{\partial f(\mathbf{x}, \mathbf{u}, 0)}{\partial \mathbf{x}}, \quad B(t) := \frac{\partial f(\mathbf{x}, \mathbf{u}, 0)}{\partial \mathbf{u}}, \quad (10)$$

$$C(t) := \frac{\partial h(\mathbf{x}, \mathbf{u})}{\partial \mathbf{x}}, \quad (11)$$

where the matrix  $\Sigma$  in (6) is the variance-covariance matrix of the disturbances of the wind field  $w(z, t)$ , i.e.,  $\Sigma = E\{w(z, t)w(z, t)^\top\} - E\{w(z, t)\}^2$ .

In the OCP (4) - (11), the confidence level  $\gamma$  is maximized while the resulting loss of generated power  $J = J(T, \mathbf{x}(T)) = -\frac{1}{T} \int_0^T F_c \dot{r} dt$  is required to be less than 20% of nominal power generation (constraint (9)). The state of the Lyapunov equation is required to satisfy  $P(0) = P(T) \succ 0$  such that open-loop stability of the solution can be guaranteed due to Lemma 1. The inequality in (8) implies the robustness of the solution w.r.t. the path constraints.

### 3.3 Stable and robust periodic trajectory assuming white noise disturbances

In this section an open-loop stable and robust trajectory is computed assuming that the disturbances are the random white noise process. This implies that the variance-covariance matrix  $\Sigma$  is the identity matrix.

For the above kite model it was possible to find an open-loop stable and robust solution of the OCP (4) - (11) with  $\Sigma = I$ . The maximal possible confidence level is  $\gamma = 2.13$ . The optimal cycle duration is  $T = 20.7$  seconds. The spectral radius of the associated monodromy matrix is  $\rho(X) = 0.86 < 1$ . Thus, the orbit is stable. The optimized robust and open-loop stable trajectory is shown in Fig. 5.

### 3.4 Stable and robust periodic trajectory assuming altitude dependent turbulence intensities

In this section an open-loop stable and robust trajectory is computed assuming that the turbulence intensities are altitude dependent and, thus, time varying throughout the kite trajectory.

The averages in time of the vertical turbulence intensities  $\sigma_x(z)$ ,  $\sigma_y(z)$  and  $\sigma_z(z)$  are shown in Fig. 6. The turbulence intensities

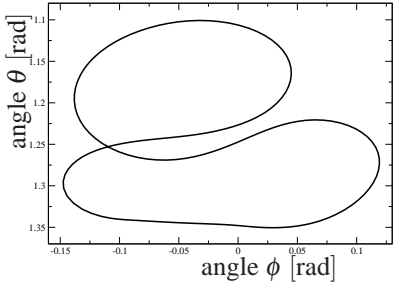


Fig. 5. Open-loop stable and robust kite trajectory in the  $\phi - \theta$  plane, considering disturbances modelled by a white noise random process

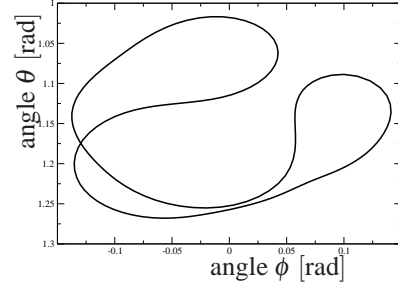


Fig. 7. Open-loop stable and robust kite trajectory in the  $\phi - \theta$  plane, considering realistic non-uniform turbulence intensities

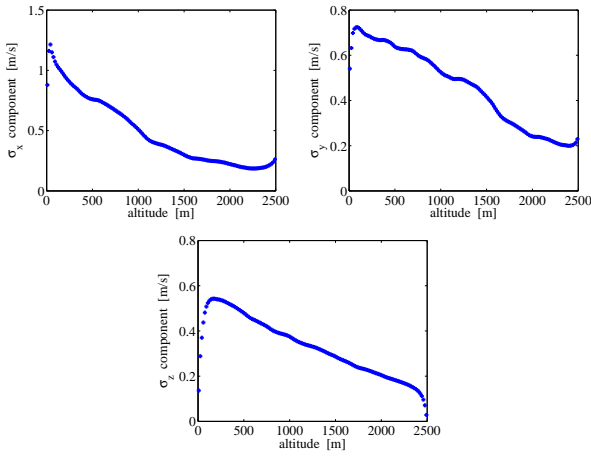


Fig. 6. Three components of the vertical turbulence intensities:  $\sigma_x$ ,  $\sigma_y$  and  $\sigma_z$

are computed as the root mean square of the velocity fluctuation ( $\tilde{v}_x, \tilde{v}_y, \tilde{v}_z$ ) in the specified direction (averaged over the time and the horizontal plane), i.e., for the fixed altitude  $z$  the turbulent intensities  $\sigma_x(z)$  are given as

$$\sigma_x(z) = \langle \tilde{v}_x \tilde{v}_x \rangle^{1/2}, \quad (12)$$

where the velocity fluctuation  $\tilde{v}_x(\vec{x}, t)$  is calculated as

$$\tilde{v}_x(\vec{x}, t) = v_x(\vec{x}, t) - \bar{v}_x(z) \quad (13)$$

for every point  $\vec{x} = (x, y, z)$  in space and for every time  $t$ . The vertical turbulent intensities  $\sigma_y(z)$  and  $\sigma_z(z)$  can be evaluated in the same way.

In order to improve the robustness of the solution from Section 3.3, the turbulence intensities from Fig. 6 are taken into account throughout the optimization procedure. The variance-covariance matrix  $\Sigma$  in this case is defined as  $\Sigma = \Sigma(z) = \text{diag} \{ \sigma_x^2(z), \sigma_y^2(z), \sigma_z^2(z) \}$ . The corresponding open-loop stable and robust trajectory as a solution of the OCP (4) - (11) is shown in Fig. 7.

The maximal possible confidence level is  $\gamma = 8.5$ . The optimal cycle duration is  $T = 24.8$  seconds. The spectral radius of the associated monodromy matrix is  $\rho(X) = 0.8 < 1$ .

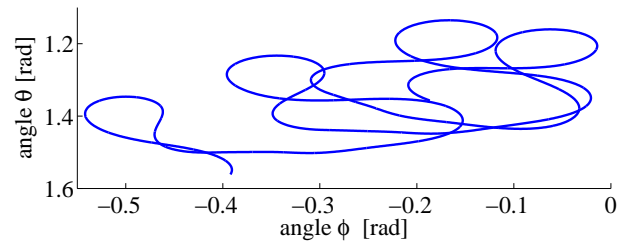


Fig. 8. Simulation of the stable and robust kite trajectory from Fig. 5 (white noise disturbances) within a turbulent time- and space-dimensional wind flow

#### 4. SIMULATION OF OPTIMAL PERIODIC KITE TRAJECTORY IN TIME DEPENDENT TURBULENT WIND FLOW

In this section the a-priori stable and robust kite trajectories computed in Sections 3.3 and 3.4 are simulated considering the realistic time- and space-dependent turbulent wind flow computed in Section 2.3.

First, the open-loop stable and robust trajectory, obtained in Section 3.3 for white noise disturbances, is simulated in a real turbulent wind flow and is visualized in Fig. 8. As predicted, the kite trajectory robustly satisfies the boundary constraints for the duration of one period, i.e., for  $t = 20.7$  seconds. The trajectory becomes non-periodic because of wind turbulences. Flying the computed trajectory in the turbulent wind flow for four periods the kite stays airborne for at least  $t = 60$  seconds.

Second, the stable and robust kite trajectory, computed in Section 3.4 where non-uniform turbulence intensities are assumed, is simulated in a real turbulent wind flow. As a result, much more stable and robust behaviour compared to the simulation in Fig. 8 is observed. This is because the confidence level  $\gamma = 8.5$  computed for the orbit in Fig. 7 is much bigger than for the one in Fig. 5, where white noise disturbances are considered. Thus, assuming non-uniform turbulence intensities throughout the OCP, more stable and robust solutions can be computed. The corresponding trajectory is simulated in the turbulent wind flow for almost seven periods and is visualized in Fig. 9. Flying this trajectory the kite stays airborne for more than  $t = 165$  seconds.

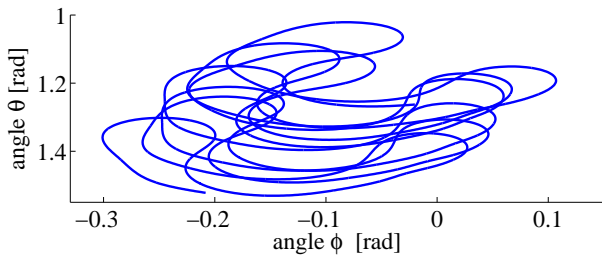


Fig. 9. Simulation of the stable and robust kite trajectory from Fig. 7 (altitude-dependent non-uniform turbulence intensities) within a turbulent time- and space-dimensional wind flow

## 5. CONCLUSIONS

In the present paper we have computed some new open-loop stable and robust trajectories for a power generating kite system. Here, we consider a realistic model for the three dimensional wind profile and different models for wind disturbances: a) uncorrelated white noise random process; b) uncorrelated bounded random process with turbulence intensities depending on the altitude. The resulting trajectories have been compared in terms of stability and robustness. The conclusion is that by assuming non-uniform, altitude-dependent turbulence intensities in the OCP, more stable and robust solutions can be computed.

As a post-processing test, both trajectories have been simulated in a real time- and space-dependent three dimensional turbulent wind flow. Flying the second trajectory, where non-uniform turbulence intensities have been considered throughout the optimization, the path constraints are satisfied for much longer time. As a consequence, the kite stays much longer airborne.

## ACKNOWLEDGEMENTS

The research was supported by the Research Council KUL via GOA/11/05 Ambiorics, GOA/10/09 MaNet, CoE EF/05/006 Optimization in Engineering (OPTEC) en PFV/10/002 (OPTEC), IOF-SCORES4CHEM and PhD-/postdoc/fellow grants, the Flemish Government via FWO (PhD/postdoc grants, projects G0226.06, G0321.06, G.0302.07, G.0320.08, G.0558.08, G.0557.08, G.0588.09, G.0377.09, research communities ICCoS, ANMMM, MLDM) and via IWT (PhD Grants, Eureka-Flite+, SBO LeCoPro, SBO Climaqs, SBO POM, O&O-Dsquare), the Belgian Federal Science Policy Office: IUAP P6/04 (DYSCO, Dynamical systems, control and optimization, 2007-2011), the IBBT, the EU (ERNSI; FP7-HD-MPC (INFOS-ICT-223854), COST intelliCIS, FP7-EMBOCON (ICT-248940), FP7-SADCO (MC ITN-264735), ERC HIGHWIND (259 166)), the Contract Research (AMINAL), the Helmholtz Gemeinschaft via viCERP and the ACCM. For the CFD simulations we used the infrastructure of the VSC - Flemish Supercomputer Center, funded by the Hercules Foundation and the Flemish Government - department EWI.

## REFERENCES

Bolzern, P. and Colaneri, P. (1988). The periodic Lyapunov equation. *SIAM J. Matrix Anal. Appl.*, 9(4), 499–512.

Calaf, M., Meneveau, C., and Meyers, J. (2010). Large eddy simulation study of fully developed wind-turbine array boundary layers. *Physics of Fluids*, 22, 015110.

Canale, M., Fagiano, L., Ippolito, M., and Milanese, M. (2006). Control of tethered airfoils for a new class of wind energy generators. In *Conference on Decision and Control, San Diego*.

Canale, M., Fagiano, L., Milanese, M., and Ippolito, M. (2007). KiteGen project: control as key technology for a quantum leap in wind energy generators. In *Proceedings of the 2007 American Control Conference*.

Diehl, M., Bock, H., and Kostina, E. (2006a). An approximation technique for robust nonlinear optimization. *Mathematical Programming*, 107, 213–230.

Diehl, M., Kühn, P., Bock, H., Schlöder, J., Mahn, B., and Kallrath, J. (2006b). Combined NMPC and MHE for a copolymerization process. In W. Marquardt and C. Pantelides (eds.), *Computer-aided chemical engineering*, volume 21B, 1527–1532. DEHEMA, Elsevier.

Houska, B. (2007). *Robustness and Stability Optimization of Open-Loop Controlled Power Generating Kites*. Master's thesis, University of Heidelberg.

Houska, B. and Diehl, M. (2007). Optimal Control for Power Generating Kites. In *Proc. 9th European Control Conference*, 3560–3567. Kos, Greece, (CD-ROM).

Houska, B. and Diehl, M. (2009). Robust nonlinear optimal control of dynamic systems with affine uncertainties. In *Proceedings of the 48th Conference on Decision and Control*. Shanghai, China.

Houska, B. and Diehl, M. (2010). Robustness and Stability Optimization of Power Generating Kite Systems in a Periodic Pumping Mode. In *Proceedings of the IEEE Multi-Conference on Systems and Control*. Yokohama, Japan.

Houska, B., Ferreau, H., and Diehl, M. (2011). ACADO Toolkit – An Open Source Framework for Automatic Control and Dynamic Optimization. *Optimal Control Applications and Methods*, 32(3), 298–312.

Houska, B., Logist, F., Impe, J.V., and Diehl, M. (2009). Approximate robust optimization of time-periodic stationary states with application to biochemical processes. In *Proceedings of the 48th Conference on Decision and Control*. Shanghai, China.

Ilzhoefer, A., Houska, B., and Diehl, M. (2007). Nonlinear MPC of kites under varying wind conditions for a new class of large scale wind power generators. *International Journal of Robust and Nonlinear Control*, 17(17), 1590–1599.

Lansdorp, B. and Ockels, W. (2005). Comparison of concepts for high-altitude wind energy generation with ground based generator. In *The 2nd China International Renewable Energy Equipment & Technology Exhibition and Conference, Beijing*.

Loyd, M. (1980). Crosswind Kite Power. *Journal of Energy*, 4(3), 106–111.

Nagy, Z. and Braatz, R. (2004). Open-loop and closed-loop robust optimal control of batch processes using distributional and worst-case analysis. *Journal of Process Control*, 14, 411–422.

Nagy, Z. and Braatz, R. (2007). Distributional uncertainty analysis using power series and polynomial chaos expansions. *Journal of Process Control*, 17, 229–240.

Ockels, W., Ruiterkamp, R., and Lansdorp, B. (2006). Ship propulsion by Kites combining energy production by Laddermill principle and direct kite propulsion. In *Kite Sailing Symposium, Seattle, USA*.

Williams, P., Lansdorp, B., and Ockels, W. (2008). Optimal Crosswind Towing and Power Generation with Tethered Kites. *Journal of Guidance, Control, and Dynamics*, 31(1), 81–92.